Dalton Transactions



PAPER

View Article Online
View Journal | View Issue



Cite this: *Dalton Trans.*, 2015, **44**, 21109

Highly tunable fluorinated trispyrazolylborates $[HB(3-CF_3-5-\{4-RPh\}pz)_3]^-$ (R = NO₂, CF₃, Cl, F, H, OMe and NMe₂) and their copper(1) complexes†

Thomas F. van Dijkman, Maxime A. Siegler and Elisabeth Bouwman*

The ethene and carbon monoxide adducts of copper(I) with seven trispyrazolylborate ligands ([HB(3-CF₃-5-{4-RPh}pz]₃]⁻; R = NO₂ (4a), CF₃ (4b), Cl (4c), F (4d), H (4e), OMe (4f) and NMe₂ (4g)) were synthesized and characterized. The ligands were synthesized from their corresponding pyrazoles and sodium tetrahydridoborate and were obtained as solvent adducts of their sodium salts after workup. When the pyrazole with the most electron-withdrawing substituent ($R = NO_2$) is used the asymmetric ligand [HB(3-CF₃-5- $(4-NO_2Ph)pz)_2(3-(4-NO_2Ph)-5-CF_3pz)]^-$ (4a') is formed as the major product. Copper(i) complexes with ethene or CO as a co-ligand were prepared in good yields and were structurally characterized using ¹H NMR, ¹³C NMR and infrared spectroscopy. Single crystal X-ray crystallography analyses revealed the structures of Na4a', Na4b, four copper ethene complexes and four copper carbonyl complexes. The structures of the copper(i) complexes show Cu^I ions in pseudo-tetrahedral coordination environments consisting of three nitrogen atoms of the trispyrazolylborate ligand and the carbonyl or η^2 -coordinated ethene ligands, with nearly identical coordination environments around the Cu^I ion. The compound [Na(4a')(H₂O)]_n crystallizes as one-dimensional chains with intermolecular $Na\cdots O_2N$ interactions. The sodium ions were found in severely distorted octahedral geometries with three nitrogen atoms from the trispyrazolylborate ligand, one agua ligand and two oxygen atoms from the nitro group of an adjacent molecule. The compound [Na₂(4b)₂(µ-H₂O)₂] crystallizes as a centrosymmetric water-bridged dimer: two five-coordinate square-pyramidal sodium ions each are coordinated facially by three nitrogen atoms from a trispyrazolylborate ligand and two bridging water ligands. Below the base of the pyramidal structure one intermolecular and two intramolecular Na···F short contacts are present. The ¹H and ¹³C NMR spectra of the copper-ethene complexes show signals for the ethene ligands in the range of 4.84-4.96 ppm and 84.9-86.8 ppm respectively. The infrared spectra of the carbonyl complexes show CO stretching frequencies in the range of 2096-2120 cm⁻¹. Both the NMR signals for the ethene ligands and infrared signals for the carbonyl ligands were found to show good correlations with the Hammett σ_0 parameters of the substituents on the phenyl rings of the ligands.

Received 13th October 2015, Accepted 12th November 2015 DOI: 10.1039/c5dt04006j

www.rsc.org/dalton

Introduction

Trispyrazolylborates (commonly referred to as scorpionate ligands¹) form a highly versatile class of ligands that were pioneered by Trofimenko in the 1960s. They have since been developed from the simple unsubstituted Tp⁻ into ligands of increasing complexity and scope.²⁻⁷ The great diversity in steric and electronic properties available in trispyrazolylborate

ligands allows for the optimization of complexes for specific purposes such as catalysis and biomimetic structural and functional models. The properties of trispyrazolylborate ligands can be changed by systematic modification of the substituents on the pyrazolyl groups or, though much less common, on the central boron atom. At present a wide variety of the facially coordinating tridentate ligands is known with substituents ranging from alkyl groups to aryl groups (both aromatic like phenyl groups and heteroaromatic such as the thienyl group) as well as phosphines, esters and amides.^{8–13} Due to the structurally and electronically similar properties of the pyrazole and imidazole rings trispyrazolylborate ligands offer an interesting avenue towards the modelling of biological systems that incorporate multiple histidine residues coordinating facially to the metal center in the active site. A metal that is encountered

^aLeiden Institute of Chemistry, Leiden University, P.O. Box 9502, 2300 RA, Leiden, the Netherlands. E-mail: bouwman@chem.leidenuniv.nl

^bDepartment of Chemistry, Johns Hopkins University, MD 21218 Baltimore, USA † Electronic supplementary information (ESI) available. CCDC 1430362–1430371. For ESI and crystallographic data in CIF or other electronic format see DOI: 10.1039/c5dt04006i

often in such sites is copper, in enzymes and proteins such as hemocyanin, cytochrome-c oxidase, ceruloplasmin, superoxide dismutase, laccase and many others. 14 Copper offers advantages besides being biologically relevant; the ethene and carbonyl complexes of copper(1) offer relatively simple systems to characterize the steric and electronic properties of novel trispyrazolylborate ligands. Such complexes have a (pseudo) tetrahedral coordination environment in which a single copper(1) ion is facially coordinated by a single trispyrazolylborate ligand and one ethene or carbonyl ligand which allows for unambiguous characterization of the steric and electronic properties of the trispyrazolylborate ligand. Unfortunately comparison of the properties of trispyrazolylborate ligands typically results in their differences being ascribed to a combination of steric and electronic factors without detailed knowledge of the contributions of each factor. To facilitate the comparison of the steric and electronic factors a series of isosteric, purely electronically varied trispyrazolylborates would be useful. By keeping the steric properties of the binding pocket around the metal center constant and varying only the electronic properties of the trispyrazolylborate ligands a spectrochemical series of isosteric trispyrazolylborate ligands could be created. Such a spectrochemical series of trispyrazolylborate ligands could be used to separately estimate the optimal electronic properties of a trispyrazolylborate ligand in a catalytic or biomimetic system prior to optimization of the steric factors. To create a spectrochemical trispyrazolylborate ligand series strict regiochemical control during ligand synthesis is required. The coordination environment around the metal must vary as little as possible while the electronic properties of the ligand are varied. In this regard trispyrazolylborate ligand synthesis offers a convenient handle in that the 3-positions of the pyrazolyl rings are typically occupied by the bulkiest substituent. Exceptions to this situation occur if the pyrazole also carries a particularly electron-withdrawing substituent like a trifluoridomethyl group, in which case the electron-withdrawing group assumes the 3-position instead. The resulting electron-withdrawing trispyrazolylborate ligands have a special place in copper(1) chemistry because they allow for the synthesis and isolation of otherwise thermally and oxidatively unstable copper(i) complexes with ligands like ethene and carbon monoxide. Examples of such ligands include [Tp^{(CF₃)2}]⁻, [Tp^{(CF₃)3}]⁻, [Tp^{CF₃,Ph}]⁻, [Ttz^{(CF₃)2}]⁻ and [Tp^{CF₃}]⁻. 15-18 The [TpCF3,RCu(C2H4)] complexes of these ligands are air stable as are the corresponding carbonyl complexes which have infrared CO stretching frequencies close to that of free CO indicating particularly electron-poor copper(1) centers. Both effects are unusual for copper(1) trispyrazolylborate complexes and can be ascribed to the electron-withdrawing effects of the fluorinated substituents on the pyrazole moieties. The trifluoridomethyl groups thus tune the electronic properties of the ligand to a great extent while adding only a limited amount of steric bulk and a chemically inert binding pocket around the copper(1) center. With the aim of synthesizing isosteric, electronically different trispyrazolylborate ligands the ligand

Table 1 Schematic representation of the ligands and complexes described in this paper, including the Hammett $\sigma_{\rm p}$ values of the substituents on the para-positions of the phenyl groups

				$[\mathbf{Tp}^{\mathrm{CF}_3,4\text{-RPh}}\mathbf{CuL}]$	
	R	$\sigma_{ m p}^{\;\;b}$	Ligand	$L = C_2H_4$	T = CO
CF ₃ N-N-CU*-L N-N-CF ₃	NO ₂ ^c CF ₃ Cl F H OMe NMe ₂	0.78 0.54 0.23 0.06 0 -0.27 -0.83	4a/4a′ 4b 4c 4d 4e 4f 4g	5a' 5b 5c 5d 5e 5f 5g	6a' 6b 6c 6d 6e 6f 6g
5a-g and 6a-g					

^aThe third pyrazole ring is schematically shown as [N=N]. ^b Taken from ref. 18. ^c The major product is an asymmetric isomer, indicated with a', see

for chemical modification of the phenyl rings while retaining the structure of the binding pocket surrounding the copper(1) center. Delocalization in the aromatic rings allows for efficient charge transfer from substituents on the distal phenyl rings to the copper(1) ion while conformational differences between the resulting complexes are limited by the steric bulk of the crowded phenyl groups. Particularly substitution on the paraposition of the phenyl rings would result charge transfer without significant structural modification to the ligands. Even though the substituents would be placed relatively far away from the copper(1) ions the charges of the substituents could be transferred quite effectively by resonance effects in the conjoined aromatic rings. In this work the effect of parasubstitution on the phenyl rings of [Tp^{CF3,Ph}] was examined; by judicious selection of electron donating and withdrawing substituents a spectroscopic series was created (Table 1). Substituents were chosen that offer a broad range of electronic properties (based on their Hammett $\sigma_{\rm p}$ parameters) and are tolerant to the strongly reducing conditions required for the synthesis of these trispyrazolylborate ligands. 19 To study the upper limit of electron withdrawing effects the particularly electron withdrawing nitro substituent was also included despite its sensitivity to reducing conditions.

Results

Synthesis

The ligands used in this work were synthesized from 4'-substituted acetophenones (1a-g) in a multistep procedure (see Scheme 1). The 4-substituted acetophenones were converted into 4'-substituted benzoyltrifluoridoacetates (2a-g) in a Claisen condensation with ethyl trifluoridoacetate in THF or diethyl ether. Typically the use of diethyl ether gave higher yields and less side products but the more polar THF was sometimes required to keep reaction mixtures from becoming too viscous.

[Tp^{CF₃,Ph}] in particular is interesting because of its potential

Dalton Transactions Paper

Scheme 1 (a) CF₃COOEt, KO^tBu/NaOEt, Et₂O, rt; (b) N₂H₄·H₂O, EtOH, reflux; (c) 3 N HCl, reflux; (d) NaBH₄, Ar either at 180 °C (melt reaction) or in refluxing 4-methylanisole.

The 4'-substituted benzoyltrifluoridoacetates were then converted into the corresponding pyrazoles (3a-g) by a two-step condensation reaction with hydrazine hydrate which resulted in product mixtures comprising the desired pyrazole and (partially) hydrated intermediates which were dehydrated by refluxing in dilute hydrochloric acid; without the additional dehydration step the reaction is typically incomplete. Alternative methods were less successful; reflux in toluene under Dean–Stark conditions required much longer reaction times and vacuum thermolysis frequently led to co-sublimation of incompletely dehydrated products. The pyrazoles can be purified readily by means of vacuum sublimation to yield pure and dry products that can be used immediately for ligand synthesis.

The pyrazoles were converted into the trispyrazolylborate ligands by heating in the presence of NaBH₄ (Scheme 1). A reaction temperature of 180 °C was used in a solvent-free reaction as reported for the synthesis of Na4e except in the cases of Na4a and Na4f for which 4-methylanisole was used as a solvent.16 In the case of Na4f the solvent was used because the melting point of 3g is too high to let the reaction proceed smoothly at 180 °C and higher temperatures led to excessive scorching. For Na4a the solvent-free synthesis resulted in the formation of large amounts of byproducts, whereas stepwise heating in 4-methylanisole facilitated the formation of the monopyrazolylborate and bispyrazolylborate intermediates at lower reaction temperatures before raising the reaction temperature to 180 °C. This was not possible without the use of a solvent as the melting point of 3a is too high (171 °C). As evident from the 1H and 13C NMR spectra of the sodium salt and the complexes of [4a] the nitro-substituted ligand formed almost exclusively as the asymmetric species in which two of the pyrazole rings have the trifluoridomethyl group in the 3-position and one pyrazole ring is attached "in reverse" with the trifluoridomethyl group in the 5-position (see Scheme 2). This asymmetric isomer will be referred to as 4a'.

All trispyrazolylborate ligands were isolated as solvent adducts of their sodium salts, typically incorporating solvents such as acetone, THF or diethyl ether in stoichiometric ratios. Instances of mixed solvent adducts were also observed such as in Na4d· $(Et_2O)_{0.5}$ (acetone)_{0.5}. Examples of similar solvent adducts in other fluorinated trispyrazolylborate ligands have been described. Na4b formed as the water adduct even when recrystallized in the presence of suitable solvents or

$$\begin{pmatrix} O_2N & CF_3 \\ N-N & N-N \\ F_3C & NO_2 \end{pmatrix}$$

Scheme 2 The asymmetric structure of the major fraction [4a']-.

mixtures thereof. All ligand salts exchanged some solvent with adventitious water upon standing in air.

The ethene and carbonyl copper(1) complexes (respectively 5a', 5b-g and 6a', 6b-g, see Table 1) were synthesized by stirring the sodium salts of the trispyrazolylborate ligands Na4a', Na4b-g and CuI in DCM in an atmosphere of ethene or carbon monoxide. It was found that if CuI was added to an ethene or carbon monoxide saturated solution of the ligand in DCM the synthesis could be performed with minimal further use of Schlenk techniques. Workup consisted of filtration to remove NaI and evaporation of the solvent in vacuo to yield the complexes as white powders which were recrystallized from DCM/pentane to yield the pure products. Most of the isolated ethene or carbonyl copper(1) complexes are air stable for at least six months in the solid state. In solution in dichloromethane 5a', 6a', 5g and 6g slowly turn green over the course of hours with associated loss of the ethene or carbonyl ligands (as evident from their NMR spectra) if exposed to air. Complexes 5b-g and 6b-g show good stability in the presence of air, light and moisture and can be manipulated without special precautions. The complexes 5a' and 6a' were found to be less stable over time and had to be kept under argon to avoid decomposition. Aside from DCM the complexes were found to be slightly soluble in n-pentane, n-hexane and cyclohexane and to have good solubility in benzene, toluene, THF, 1,4-dioxane, chloroform and acetonitrile. A general trend appears to be that the more polar complexes (those incorporating methoxy and dimethylamino substituents) are less soluble in the more apolar solvents although even 5g and 6g are somewhat soluble in *n*-hexane. Coordinating solvents (acetonitrile, acetone and THF) cause decomposition of the complexes over

Table 2 Selected bond distances (Å) and angles (°) for Na4a' and Na4b

Bond distances (Å)	Na4a′	Na4 b	Bond angles (°)	Na 4a ′	Na 4b
Na1-N12	2.4731(15)	2.4595(12)	O1W-Na1-O1W'		82.03(4)
Na1-N22	2.4351(15)	2.4440(12)	O1W-Na1-N12	99.18(6)	104.30(4)
Na1-N32	2.5737(15)	2.4355(12)	O1W-Na1-O231'	86.28(6)	101100(1)
Na1-O1W	2.2581(16)	2.4512(12)	O1W-Na1-O232'	67.35(5)	
Na1-O1W'		2.4274(12)	O1W'-Na1-N12	21.12.(2)	100.89(4)
N11-N12	1.3566(19)	1.3605(14)	O1W'-Na1-N32		99.69(4)
N21-N22	1.3603(18)	1.3589(15)	O1W-Na1-N22	103.78(6)	104.57(4)
N31-N32	1.3551(19)	1.3590(15)	N22-Na-N32	81.30(5)	73.79(4)
Na1···F12	3.625(2)	-1000 (-0)	N12-Na-F13'	(-)	162.1(3)
Na1···F13′	(-)	2.930(12)	O231'-Na1-O231'	46.64(4)	(-)
Na1···F21′	4.144(1)	21300(12)	0201 1101 0201	10.01(1)	
Na1F23	(1)	3.197(4)			
Na1F33		3.116(2)			

the course of hours to days; decomposition is slowest for the most Lewis acidic complexes.

Single crystal X-ray crystallography

Colorless single crystals of Na4a', Na4b, 5b, 5c, 5d, 5f, 6b, 6c, 6d and 6f were obtained by slow evaporation of DCM solutions at -20 °C and were characterized by single crystal X-ray crystallography. Crystallographic data are given in Tables S1-S3.† Selected distances and bond angles are given in Table 2 for the sodium salts of 4a' and 4b, in Table 3 for the ethene complexes, and in Table 4 for the carbonyl complexes. Projections of the structures of Na4a' and Na4b are shown in Fig. 1 and 2. As representative examples of the copper(i) complexes projections of the structures of 5b and 6b are shown in Fig. 3; projections of the other structures are provided in the ESI.†

Na4a' crystallized as a coordination polymer with bridging $NO_2 \cdots Na^+$ interactions (with bidentate κ^2 -O,O' coordination). The sodium ions are in a severely distorted octahedral coordination sphere comprising three nitrogen atoms from the ligand 4a', two oxygen atoms from a nitro group of an adjacent complex and a water molecule, which is stabilized by hydrogen bridges to the nearby nitro group oxygen atoms. The Na-N distances range from 2.4351(15) to 2.5737(15) Å, the Na-O_{aqua} distance is 2.25581(16) Å and the Na-O₂N distances are 2.5291 (14) and 2.8633(14) Å. The severely distorted octahedral coordination sphere on the sodium ion in Na4a' appears to be complemented by an intramolecular Na···FC contact between the sodium ion and a nearby trifluoridomethyl group. The upper limit to what may be considered as short contacts (and thus potentially dative bonds) between a hard donor/acceptor pair such as sodium ions and fluorine atoms in fluoridocarbons is somewhat vague as it depends on the ionic and covalent radii that are used. Using the ionic radius of six-coordinate Na⁺ ions reported by Shannon et al. (1.02 Å) Plenio et al. suggested an upper limit to the interatomic distance between Na⁺ ions and fluorine atoms in fluoridocarbons at 3.07 Å. 22,23 It was further pointed out that Na···FC contacts typically have shallow potential wells, which means small outside forces such as those present in crystals because of packing can cause significant

Table 3 Selected bond distances (Å) and angles (°) for complexes 5b, 5c, 5d and 5f^a

Bond distances (Å)							
	5 b	5 c	5d	5f			
C=C _{ethene}	1.357(4)	1.311(14)	1.350(3)	1.351(8)			
Cu-C _{ethene}	2.034(2)	2.019(9)	2.0428(16)	2.054(5)			
	2.051(5)	2.035(9)	2.0455(16)	2.046(5)			
Cu-N12	2.0450(15)	2.094(3)	2.0255(14)	2.026(4)			
Cu-N22	2.0369(15)	2.070(3)	2.0164(13)	2.046(4)			
Cu-N32	2.2465(16)	2.137(4)	2.2964(13)	2.224(4)			
N11-N12	1.3626(19)	1.356(5)	1.3685(17)	1.360(5)			
N21-N22	1.3619(19)	1.355(5)	1.3648(17)	1.363(6)			
N31-N32	1.3631(19)	1.363(5)	1.3682(17)	1.358(5)			
N11-B1	1.553(2)	1.558(5)	1.553(2)	1.564(5)			
N21-B1	1.554(2)	1.561(5)	1.552(2)	1.539(6)			
N31-B1	1.545(2)	1.537(6)	1.545(2)	1.551(6)			

Bond angles (°)

	5 b	5c	5d	5f
C-Cu-C	38.79(11)	37.7(4)	38.55(7)	38.5(2)
Cu-C=C	71.3(2)	70.5(5)	70.83(10)	70.5(3)
	69.9(2)	71.8(5)	70.62(10)	71.1(3)
N12-Cu1-N22	92.55(6)	89.58(14)	90.77(5)	94.64(15)
N22-Cu1-N32	87.03(6)	90.60(13)	90.77(5)	88.25(14)
N12-Cu1-N32	89.81(5)	90.17(13)	85.68(5)	87.01(14)
C1-Cu1-N12	149.26(9)	126.2(4)	115.04(7)	148.49(18)
C1-Cu1-N22	112.92(9)	111.5(3)	147.96(7)	110.75(18)
C1-Cu1-N32	107.70(9)	135.8(4)	108.95(7)	111.30(18)
C2-Cu1-N12	111.18(9)	111.8(3)	151.13(6)	110.68(18)
C2-Cu1-N22	147.41(11)	148.9(3)	111.15(6)	144.25(19)
C2-Cu1-N32	114.02(12)	110.8(3)	111.57(̈́7)́	116.93(18)

^a Bond distances and bond angles are only provided for one of the two crystallographically independent molecules.

changes to the interatomic distance between the sodium ion and the fluorine atom. The distances observed for the Na···FC contacts in Na4a' are 3.625(2) Å and 4.144(1) Å, considerably longer than the upper limit of 3.07 Å even when crystal packing effects are taken into account. The proximity of the trifluoridomethyl groups is therefore not considered to constitute

Table 4	Selected	bond	distances	(Å)	and	angles	(°)	for	complexes	6b,
6c . 6d an	nd 6f ^a									

	6b	6c	6d	6f
C1-O11	1.124(2)	1.126(4)	1.123(8)	1.130(4
Cu1-C1	1.7998(19)	1.800(3)	1.791(6)	1.793(3
Cu-N12	2.0642(15)	2.069(2)	2.0552(19)	2.038(2
Cu-N22	2.0496(15)	2.056(2)	` '	2.062(2
Cu-N32	2.0505(15)	2.057(3)		2.075(2
N11-N12	1.3571(19)	1.354(3)	1.364(2)	1.353(3
N21-N22	1.3623(19)	1.358(3)		1.367(3
N31-N32	1.3625(19)	1.360(3)		1.358(3
N11-B1	1.548(2)	1.553(3)	1.553(2)	1.560(3
N21-B1	1.557(2)	1.549(3)	. ,	1.554(3
N31-B1	1.553(2)	1.546(4)		1.554(3

Bond angles (°)

Dalton Transactions

	6b	6c	6d	6f
Cu1-C1-O11	176.0(2)	177.4(3)	180.0	178.3(3)
C1-Cu1-N12	118.66(8)	122.17(11)	125.13(5)	126.66(11)
C1-Cu1-N22	129.95(8)	127.99(11)		121.77(12)
C1–Cu1–N32	126.11(7)	124.75(13)	90.19(7)	125.74(11)
N12–Cu1–N22	90.60(6)	90.14(9)		91.65(8)
N22-Cu1-N32	88.85(6)	90.58(8)		90.23(7)
N32-Cu1-N12	91.85(6)	90.37(8)		90.31(8)

^a Bond distances and bond angles are only provided for one of the two crystallographically independent molecules.

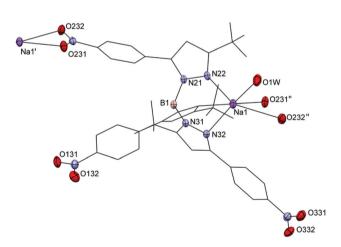


Fig. 1 Projection of part of the structure of [Na(4a')(H₂O)]_n with displacement ellipsoids plotted at the 50% probability level at 110(2) K. For clarity major parts of the ligand are shown in wireframe and hydrogen atoms have been omitted. Symmetry operations ' = $\left[\frac{2}{3} - x, y - \frac{1}{2}, \frac{2}{3} - z\right]$, " = $\left[\frac{2}{3} - x, y + \frac{1}{2}, \frac{2}{3} - z\right]$.

actual bonding between the sodium ion and the fluorine atoms but merely dipolar interactions.

Na4b crystallized as a dimer comprising two sodium ions in distorted square-pyramidal coordination geometries. The sodium ions are each coordinated facially by three nitrogen atoms of the trispyrazolylborate ligand and by two bridging water molecules (O_{aqua}). The Na-N distances range from 2.4355(12) Å to 2.4595(12) Å and the Na-O_{aqua} distances are 2.4274(12) Å and 2.4512(12) Å. trans to the apical position are one intermolecular and two intramolecular Na···FC short contacts, at distances of respectively 2.930(12), 3.197(4) and 3.116(2) Å. With the foregoing considerations regarding Na...FC short contacts in mind it appears reasonable to consider both the intermolecular and intramolecular Na···FC distances in the structure of Na4b as short contacts.

The crystal structures of Na4a' and $[Na(4e)(H_2O)]_n$ contain non-bridging water ligands while the crystal structures of Na4b and $[Na_2(Tp^{{\rm \overline{CF}_3},{\rm CH}_3})_2(\mu\text{-}H_2O)_2]$ are dinuclear and contain bridging water molecules. The Na-O_{aqua} distance in the crystal structure of Na4a' of 2.2558(16) Å is comparable to the distance observed in $[Na(4e)(H_2O)]_n$ (2.245(2) Å) but shorter than the distance in $[Na_2(Tp^{CF_3,CH_3})_2(\mu-H_2O)_2]$ (2.417(2) Å), which is closer to the Na-O_{aqua} distance found in Na4b (2.4274(12) Å and 2.4512(12) Å).16

Complexes 5b, 5c, 5d, 5f, 6b, 6c, 6d and 6f all have highly similar coordination environments around the copper(1) center. In every case the copper(1) center is coordinated by three nitrogen atoms from the trispyrazolylborate ligand and either the carbon atom of the carbonyl ligand or the ethene ligand in the typical η^2 coordination. Bond lengthening or contraction in the carbonyl and ethene ligands as a result of π -backbonding interactions are not evident from the bond lengths observed in the crystal structures and are assumed to be obscured by crystal packing effects. The Cu-N distances in the ethene complexes (5b, 5c, 5d and 5f) range from 2.0164(13) to 2.2964(13) Å with in all cases two shorter bonds (2.0164(13)-2.094(3) Å) and one longer bond (2.173(4)-2.2964(13) Å); such asymmetry in the Cu-N bond lengths was also observed in other [Cu^I(Tp^{R,R'})(C₂H₄)] complexes. ^{24,25} The Cu-N bond lengths in the carbonyl complexes (6b, 6c, 6d and 6f) fall in the range 2.038(2) Å-2.075(2) Å and do not feature the two ranges of Cu-N bond lengths observed in the ethene complexes. The unequal Cu-N bond lengths in the ethene complexes are attributed to the symmetry of ethene. Ethene ligands have a two-fold symmetry while the carbonyl ligands have full rotational symmetry. This means that while the carbonyl copper complexes can retain the approximate threefold symmetry of the trispyrazolylborate ligand, whereas the ethene complexes cannot. The resulting pseudo-twofold symmetry observed in the solid state of the ethene complexes means that π-backbonding into the π* orbitals of the ethene ligands can not occur with equal contributions from all of the pyrazole rings but mostly from two of the three rings. The resulting discrepancy in charge transfer from the rings to the π^* -orbitals of the ethene ligand explains the presence of two short Cu-N bonds and one long Cu-N bond in complexes 5b-g. The compounds 6b, 6c and 6f crystallized with pseudo threefold rotational symmetry with Cu-C-O angles ranging from 176.0(2) to 178.3(3)°. Complex 6d crystallized with proper threefold rotational symmetry. The elongated thermal ellipsoid for the oxygen atom of the carbonyl ligand suggests that this ligand is most likely disordered as the C=O bond may not be perfectly aligned along the threefold axis. The deviation from

Paper Dalton Transactions

Fig. 2 Projection of the structure of [Na₂(4b)₂(μ-H₂O)₂] with displacement ellipsoids plotted at the 50% probability level at 150(2) K. For clarity major parts of the ligand are shown in wireframe and hydrogen atoms have been omitted. Symmetry operation ' = [-x, 1-y, -z].

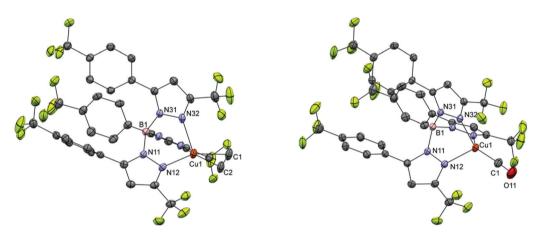


Fig. 3 Projections of the structures of 5b (left) and 6b (right) with displacement ellipsoids plotted at the 50% probability level at 110(2) K. For clarity hydrogen atoms have been omitted. Projections of the structures of the other ethene and carbonyl complexes are available in the ESI.†

rotational symmetry in 6b, 6c and 6f is small and might be the result of crystal packing effects.

NMR spectroscopy

The ¹H and ¹³C-NMR spectra of compounds 5a', 5b-g and 6a', 6b-g were recorded in deuterated DCM as it was found to be the only solvent in which the ethene complexes are all soluble and air-stable over longer periods of time (more than 30 minutes). CDCl₃, acetone- d_6 , THF- d_8 , benzene- d_6 and DMSO d_6 caused solutions of the copper ethene compounds to turn green after some time. The coordinating solvents DMSO- d_6 , acetone- d_6 , THF- d_8 and benzene- d_6 (a π -donor solvent) all appeared to be competing with the ethene ligands as peaks for free ethene grow over time on ¹H NMR. The complexes with the less Lewis basic trispyrazolylborate ligands are more stable in solution. Complexes 5b-g gave very similar spectra with no evidence of anisotropy in the signal for the ethene ligand at room temperature. Considering the asymmetry observed in the crystal structures of complexes 5b-g splitting of the ethene peaks or at least some peak broadening could be expected. The absence of

such effects appears to indicate fluxional behavior of the ethene ligand within the NMR timescale. In the NMR spectra of 5b-g the ethene ligands were detected as sharp singlets with chemical shifts between 4.81 and 4.96 ppm which are upfield from the chemical shift of free ethene (5.40 ppm in DCM- d_2) but not as far upfield as the signals observed in complexes of non-fluorinated trispyrazolylborate ligands like $[Tp^{Me_2}Cu(C_2H_4)]$ (4.41 ppm in DCM- d_2). The ethene protons of 5a' showed as a singlet at 4.44 ppm which was assigned to the asymmetric isomer; a small singlet at 4.99 ppm in the same spectrum was tentatively assigned to the ethene protons of the complex 5a incorporating the symmetric isomer [4a]. The ratio of the integrals of the ethene protons of the symmetric 5a vs. the asymmetric species 5a' was approximately 1:20. In all ethene complexes peak broadening in the presence of free ethene was not observed, indicating that the exchange of coordinated ethene, if at all, does not occur within the NMR time scale. Solutions of all ethene complexes in DCM- d_2 show no peak for free ethene even upon prolonged standing. The 1H-NMR signals for the borohydrides were

Dalton Transactions Paper

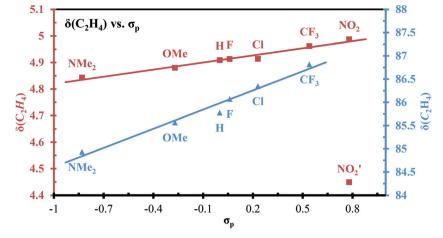


Fig. 4 1 H chemical shifts (squares, red trend line. 5a' was not included in the trend line) and 13 C chemical shifts (triangles, blue trend line) of the ethene ligands vs. the Hammett $\sigma_{\rm p}$ parameters of the substituents on the trispyrazolylborate ligands in complexes 5a–g and 5a'.

observed in the sodium compounds Na4a–g as well as the carbonyl and ethene complexes as broadened singlets with chemical shifts in the range 4.3–4.9 ppm. In principal the resonances of the borohydrides should be present as overlapping quartets and smaller septets as a result of splitting by 10 B (I=3) and 11 B (I=3/2). Typically, however, these resonances are observed as (broadened) quartets only in relatively symmetric environments. In less symmetric environments the quadrupoles of the boron nuclei are more pronounced and the borohydride resonances broaden to broad singlets without distinguishable splitting as is the case in this work. 27

In the 13 C-NMR spectra of complexes **6a**′ and **6b–g** no signals were observed for the CO ligands even after increasing the relaxation delay; we ascribe the lack of signals for CO to the low natural abundance of 13 CO and peak broadening. 28,29 The shifts of the resonances trispyrazolylborate ligands show only small differences between the ethene and the carbonyl complexes. For complexes **5b–g** the change in the 1 H-NMR and 13 C-NMR shifts of the ethene protons and carbon atoms respectively is linearly correlated with the $\sigma_{\rm p}$ values of the *para*-substituents on the phenyl groups ($R^2 = 96\%$ for 1 H and $R^2 = 97\%$ for 13 C; see Fig. 4).

Infrared spectroscopy

The IR spectra of complexes 5a', 5b-g and 6a', 6b-g were recorded in the solid state at 1 cm⁻¹ resolution. Complexes 6a', 6b-g have CO stretching frequencies in the range 2096-2120 cm⁻¹, close to that of free CO (2143 cm⁻¹). This indicates that the compounds have relatively Lewis-acidic copper(i) ions compared to other, similar, copper(i) carbonyl complexes like [Tp^{Me2}CuCO] (2066 cm⁻¹) and [Tp^{Ph2}CuCO] (2080 cm⁻¹, see Table 5 for more examples). The CO stretching frequencies correlate linearly ($R^2 = 95\%$) with the σ_p values of the substituents on the phenyl rings for compounds, with the exception of 6a' and 6g (see Fig. 5). For complex 6a' this is likely because the structure of $[4a']^-$ is asymmetric and thus poorly comparable to the other ligands in the series, in

analogy with the ethene resonances in the NMR spectra of compound 5a'. The CO stretching frequency observed in complex 6g is significantly higher than the value predicted based on the trend line in Fig. 5 (approximately 2076 cm⁻¹) for which no obvious explanation is available. Possibly unusual crystal packing effects cause the CO stretching frequency to be different than predicted, but as all attempts to grow crystals failed this hypothesis remains untested. Unfortunately infrared measurements on a sample of 6g in DCM were inconclusive as no clear signal was observed until evaporation caused solid 6g to precipitate. CO stretching typically shows itself in infrared spectroscopy as sharp absorptions due to the symmetry of the vibration. One possible explanation for the absence of an obvious CO stretching peak in solution is a lowering of the symmetry of the bonding environment surrounding the carbonyl ligand. Such lowering of local symmetry could be the result of out-of-axis vibrations of the carbonyl ligand, somewhat similar to motion of the ethene ligands in the NMR experiments and presumably have similarly low barriers. We surmise that liberation of the carbonyl ligand from the copper ion is considerably more pronounced in solution compared to the solid state and that as a result peak broadening causes the weak signal to be drowned out by noise.

The B–H moieties of the trispyrazolylborate ligands feature IR stretching frequencies that are typically found as small, broad peaks around 2600 cm $^{-1}$ (see Table 5 and Fig. 5) in Lewis-basic trispyrazolylborate complexes. In order to compare the B–H stretching frequencies of ligands **4a–g** the carbonyl complexes **6a**′ and **6b–g** and other, structurally similar, carbonyl complexes were compared. The pseudo-threefold axial symmetries observed in such carbonyl complexes mean that the comparison is not likely to be distorted by local asymmetry. The B–H stretching frequencies of complexes **6a**′ and **6b–g** were observed in the region 2611–2647 cm $^{-1}$. The B–H stretching frequencies show considerably less linearity vs. the σ_p parameters of the substituents of the trispyrazolylborate ligands

Table 5 Selected 1 H and 13 C chemical shifts and bond lengths for the compounds 5a-g and 6a-g, L = C₂H₄ or CO

	$C_2H_4^a$ (pp	om)					
Compound	¹³ C	¹ H	$\nu_{\mathrm{CO}}\mathrm{(cm^{-1})}$	$\nu_{\mathrm{BH}}^{\ f}(\mathrm{cm}^{-1})$	C=C (Å)	C≡O (Å)	Ref.
Free C ₂ H ₄ /CO	123.2	5.40	2143		1.3384(10)	1.13078(9)	30, 31
$[Tp^{(CF_3)2}CuL]$	89.1^{b}	4.96^{b}	2137	2634	1.325(9)	1.110(5)	18, 20, 32
$[Cu(4a')L]^d$	86.4	$4.44 (4.99^e)$	2105	2611			This work
[Cu(4b)L]	86.8	4.96	2120	2620	1.342(3)	1.124(2)	This work
[Cu(4c)L]	86.4	4.91	2113	2616	1.340(9)	1.126(4)	This work
[Tp ^{CF₃,Me} CuL]			2107	2575		1.122(3)	33
[Cu(4d)L]	86.1	4.91	2103	2616	1.350(3)	1.123(8)	This work
[Tp ^{CF₃,Ph} CuL]	85.8	4.91	2101	2639	1.30(1)	1.113(5)	This work, 16
[Tp ^{CF₃} CuL]	85.8^{c}	4.89^{c}	2100	2507	1.34(1)	1.126(5)	18,20
[Cu(4f)L]	85.6	4.81	2096	2636	1.351(8)	1.130(4)	This work
[Cu(4g)L]	84.9	4.84	2096	2647			This work
[Tp ^{Me₂} CuL]		4.41	2066	2500	1.329(9)		26,34
[Tp ^{Ph2} CuL]	81.6^{b}	3.53	2080	2635	1.381(19)	1.08(1)	8,35

 $[^]a$ DCM- d_2 . b CDCl₃. c C₆D₆. d Asymmetric isomer. e Symmetric isomer. f As observed in the Cu(i) CO complexes.

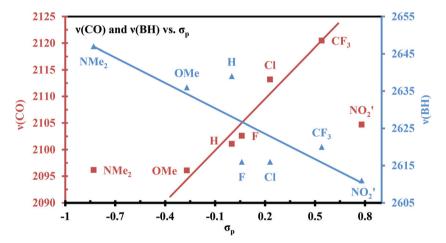


Fig. 5 Infrared CO stretching frequencies (red squares) and BH stretching frequencies (blue triangles) of complexes 6a', 6b-g vs. the Hammett σ_p parameters of the substituents on the trispyrazolylborate ligands. The red linear trend line was calculated including all points except 6a' and 6g ($R^2 = 0.95$). The blue linear trend line was calculated including all complexes 6a', 6b-g ($R^2 = 0.74$).

4a' and 4b-g ($R^2 = 0.74$) than the CO stretching frequencies. Intriguingly, compared to the unexpectedly high CO stretching frequency the B-H stretching frequencies of 6a' and 6g appear almost exactly on the trend line in Fig. 5. The most Lewis-basic trispyrazolylborate ligands have the highest B-H stretching frequencies as donation of electron density towards the borohydride increase the strength of the hydridic bond.

Discussion

In this work seven new fluorinated trispyrazolylborate ligands ($[Tp^{CF_3,4\text{-RPh}}]^-$, $R = NO_2$, CF_3 , Cl, F, H, MeO and NMe_2) and their copper(i) complexes with carbon monoxide and ethene were prepared. The ligands form an isosteric spectrochemical series based on the electronic properties of the substituents placed on the 4-position of the phenyl rings. The pyrazoles

3a–g were readily prepared from ethyl trifluoridoacetate and 4'-substituted acetophenones using a Claisen condensation, followed by cyclization with hydrazine. The synthesis of the trispyrazolylborate ligands requires fine-tuning of the conditions depending on the specific pyrazole using solventless reactions whenever possible; 4-methylanisole was used as a solvent if temperature control was required or the melting point of the pyrazole was too high. To the best of our knowledge [4a']⁻ is only the second example in the literature of a trispyrazolylborate ligand to include the synthetically challenging nitro group, the first being [Tp^{NO2}]⁻.³⁶

The trispyrazolylborate ligands studied in this work all formed as their symmetric isomers with the trifluoridomethyl groups in the 3-positions of the pyrazole rings, except [4a'] which formed as a mixture of symmetric and asymmetric species. The major product was the asymmetric species in which one of the pyrazole rings is connected to the boron

center with the nitrogen atom adjacent to the phenyl ring. The regioselectivity usually observed in the synthesis of trispyrazolylborate ligands is a result of the relative steric and electronic properties of the substituents on the 3 and 5 positions of the pyrazole, which influence the nucleophilicity of the nitrogen atoms. Typically the bulkiest substituent assumes the 3 positions of the pyrazole rings in the trispyrazolylborate anion. However, if one of the substituents is considerably more electron withdrawing than the other it will assume the 3 position even if the other substituent is bulkier. This regioselectivity is pronounced in ligands with clearly sterically or electronically differentiated substituents like $[Tp^{Ph,Me}]^-$, $[Tp^{CF_3,Me}]^-$ and $[Tp^{CF_3}]^-$ but breaks down when the steric and electronic differences are small such as in $[Tp^{iPr,Me}]^-$ which formed a 4:1 mixture of symmetric and the asymmetric isomers.³⁷ Evi-

dently the strongly electron withdrawing nitro group in [4a']

causes the electronic disparity between the trifluoridomethyl groups and phenyl rings to diminish sufficiently to shift the thermodynamic equilibrium of the system so that the asym-

metric isomer is favored over the symmetric isomer. The absence of the formation of asymmetric isomers in the other

ligands in the series puts an upper limit on the σ_p parameter

of the substituents that can be used to synthesize symmetric

Dalton Transactions

 $\mbox{[Tp}^{\mbox{CF}_3,4\mbox{R-Ph}]$^-$ ligands between +0.54 (CF}_3) and +0.78 (NO}_2).$ The good correlation between the chemical shifts of the ethene protons in complexes 5b-g vs. σ_p of the substituents on the phenyl rings of the ligands was used to predict the chemical shift of the ethene protons of the symmetric complex 5a. Based on the trend line in Fig. 4 and the σ_p parameter of the nitro group the signal for the symmetric complex 5a was predicted to be around 4.98 ppm and indeed a weak singlet was found at 4.99 ppm. Comparison of the integrals of the ethene protons in the symmetric and asymmetric complexes gave an approximate 1:20 ratio. Unfortunately attempts to locate the infrared CO stretching frequency of the symmetric isomer of **6a** using the σ_p parameter of the nitro group and the trend line in Fig. 5 were unsuccessful as the predicted CO stretching frequency for the symmetric isomer 6a at 2128 cm⁻¹ would be obscured by the much stronger absorption at 2105 cm⁻¹ of the asymmetric isomer 6a'.

More difficult to explain is the unexpectedly high CO stretching frequency observed for $6\mathbf{g}$, which was predicted to be at 2076 cm⁻¹ but instead was found at 2096 cm⁻¹, the same value as found for $6\mathbf{f}$. It appears implausible that the CO stretching frequencies of $6\mathbf{f}$ and $6\mathbf{g}$ are equal as an effect of equal amounts of π -backbonding interactions as the ¹H and ¹³C chemical shifts of the ethene ligands in $5\mathbf{f}$ and $5\mathbf{g}$ almost exactly conform to the predicted values. Unfortunately the higher than expected CO stretching frequency of $6\mathbf{g}$ cannot be conclusively explained by crystal packing effects as infrared spectroscopy on $6\mathbf{g}$ in solution was inconclusive and all attempts at crystallization failed.

With the exceptions of **6a** and **6g** the predictability of the chemical shifts of the ethene protons in the ethene complexes and CO stretching frequencies in the carbonyl complexes with respect to the $\sigma_{\rm p}$ parameters of the substituents of the phenyl

rings in the trispyrazolylborate ligands is excellent. The ability of the ligands to propagate the electron donating or withdrawing effects of the substituents on the phenyl rings over as many as eight bonds and almost one nanometer, is remarkable. The explanation for these long range effects is found in the ability of the ligands to propagate charges by means of resonance structures. Further underscoring the importance of resonance effects is the observation that the B-H stretching frequencies observed in the carbonyl complexes 6a' and 6b-g are much less predictable than the CO stretching frequencies because the nitrogen atom adjacent to the borohydride is not part of these resonance structures. We conclude that indeed the π -backbonding ability of the copper(1) centers can be modified extensively through substitution of the trispyrazolylborate ligands without significantly affecting the steric properties of the binding pocket surrounding the metal center.

Conclusions

In this work the synthesis and characterization of copper(1) complexes comprising a spectrochemical series of trispyrazolylborate ligands and ethene or carbon monoxide have been described. The ethene and carbonyl complexes described in this work are essentially isostructural around their copper(1) centers while their electronic properties vary significantly and predictably based on the Hammett σ_p parameters of the substituents placed on the trispyrazolylborate ligands. The spectroscopic data reveal good correlations between the chemical shifts of the ethene protons and CO stretching frequencies vs. the Hammett $\sigma_{\rm p}$ parameters. Notable exceptions to the, otherwise predictable, compounds in this work were the ligand [4a'] and the carbonyl complex 6g. The ligand [4a'] formed almost exclusively as an asymmetric isomer with one of the pyrazole rings counter-rotated so as to have its 4'-nitrophenyl substituent in the 3-position instead of the trifluoridomethyl group. We attribute the asymmetry of [4a'] to the strongly electron withdrawing properties of the nitro group. Copper complex 6g shows a surprisingly high CO stretching frequency. That this aberrant result is not due to trend-breaking properties of the ligand is evident from the good correlation between the predicted and found values in the corresponding ethene complex 5g. The results presented in this work underscore the usefulness of combining the use of more than a single ancillary ligand probe with the systematic study of this promising and important class of ligands.

Experimental

General information

All manipulations of air-sensitive compounds were performed in an atmosphere of purified argon gas using standard Schlenk techniques. All solvents were purchased from commercial sources and reagent grade. Solvents used for airsensitive manipulations were dried and deaerated using a

PureSolv MD 5 Solvent Purification System and stored on 3 Å molecular sieves under argon. When appropriate, glassware was flame dried in vacuo immediately prior to use. ¹H and ¹³C NMR spectra were recorded on a Bruker DPX300 spectrometer (300 MHz for ¹H and 75.44 MHz for ¹³C); Bruker DMX400 spectrometer (400 MHz for ¹H and 100.6 MHz for ¹³C); Bruker Avance AV500 spectrometer (500 MHz for ¹H, 160 MHz for ¹¹B and 126 MHz for ¹³C) or Bruker Avance 600 (600 MHz for ¹H, 193 MHz for ¹¹B and 151 MHz for ¹³C). Chemical shifts are given in ppm and referenced using the deuterated solvents as internal references for ¹H and ¹³C. ³⁸ ¹³C spectra were recorded using ¹H-decoupling. Elemental analyses were performed using a Perkin Elmer 2400 series II CHNS/O analyzer or by the Microanalytical laboratory Kolbe in Germany. IR spectra were recorded on a Perkin Elmer UATR Two FT-IR spectrometer set to a resolution of 1 cm⁻¹. HRMS spectra were recorded on a Thermo Scientific LTQ Orbitrap XL high resolution FT-MS system in MeCN. Intermediates 2a, 2b, 2d and 2f were synthesized according to a literature procedure using KOt-Bu in THF instead of sodium in methanol.³⁹ 2d was purified by conversion to the copper(II) diketonate instead of column

Single crystal X-ray crystallography

chromatography as described below.

All reflection intensities were measured at 110(2) K or 150(2) K (only for Na4b) using a SuperNova diffractometer (equipped with Atlas detector) with Cu K α radiation ($\lambda = 1.54178 \text{ Å}$) under the program CrysAlisPro (Versions 1.171.36.32/1.171.37.31 Agilent Technologies, 2013/2014). The same program CrysAlis-Pro was used to refine the cell dimensions and for data reduction. All structures were solved with the program SHELXS-2013/2014 (Sheldrick, 2008) and were refined on F² with SHELXL-2013/2014.⁴⁰ Analytical numeric absorption corrections based on a multifaceted crystal model were applied using CrysAlisPro. The temperature of the data collection was controlled using the system Cryojet (manufactured by Oxford Instruments). The H atoms were placed at calculated positions (unless otherwise specified) using the instructions AFIX 43 with isotropic displacement parameters having values 1.2 times $U_{\rm eq}$ of the attached C atoms. The H atoms attached to C1/C2, C3/C4 (ethene), and to B1 and B2 were found from difference Fourier maps, and their atomic coordinates were refined freely. The H atoms attached to the water molecules (only for Na4a' and Na4b) and to the B atoms were found from difference Fourier maps, and their coordinates were refined freely using the DFIX instructions. For 5b, 5c, 5d and 5f, the C-H and H.··H distances of the ethene molecules were restrained using the DFIX instructions. Their isotropic temperature factors were fixed for the ethene molecules (1.2 times $U_{\rm eq}$ of the attached C atoms).

Na4a′. The structure is ordered. CCDC 1430370 contains the supplementary crystallographic data for Na4a′.

Na4b. The structure is partly disordered. The six -CF₃ groups are found disordered over two or three orientations. All occupancies factors can be retrieved from the cif file. When crystals of Na4b were flash cooled from RT to 110 K, the

crystal shattered (most likely due to a solid-solid phase transition), resulting to poor quality diffraction. When crystals were cooled from RT to 150 K, the crystals remained stable. CCDC 1430371 contains the supplementary crystallographic data for Na4b.

[Cu(4b)(C₂H₄)] (5b). The structure is mostly ordered. The asymmetric unit contains two crystallographically independent molecules. One of the two crystallographically independent ethene molecules is found to be disordered over two orientations, and the occupancy factor of the major component of the disorder refines to 0.849(5). As the H atoms of the minor component could not be retrieved *via* difference Fourier map, the H atoms of the major component were constrained to have full occupancies. CCDC 1430362 contains the supplementary crystallographic data for 5b.

 $[Cu(4c)(C_2H_4)]$ (5c). The structure is mostly ordered. The asymmetric unit contains two crystallographically independent molecules. One of the two crystallographically independent ethene molecules is found to be disordered over two orientations, and the occupancy factor of the major component of the disorder refines to 0.502(7). The crystal is racemically twinned, and the BASF scale factor refines to 0.510(14). CCDC 1430363 contains the supplementary crystallographic data for 5c.

 $[Cu(4d)(C_2H_4)]$ (5d). The structure is ordered. CCDC 1430364 contains the supplementary crystallographic data for 5d.

[Cu(4f)C₂H₄] (5f). The structure is mostly ordered. The asymmetric unit contains two crystallographically independent molecules. One of the two crystallographically independent ethene molecules is found to be disordered over two orientations, and the occupancy factor of the major component of the disorder refines to 0.56(3). The positions of the H atoms for the disordered ethene molecule are most likely smeared out, and cannot be retrieved reliably from the data collected. The crystal is racemically twinned, and the BASF scale factor refines to 0.43(3). The riding model AFIX 93 could not be used as this will put the H atoms along the plane defined by Cu2, C3 and C4, which is chemically impossible (the H atoms must be approximately located in the plane perpendicular to the plane defined by Cu2, C3 and C4). CCDC 1430365 contains the supplementary crystallographic data for 5f.

[Cu(4b)CO] (6b). The structure is mostly ordered. One $-CF_3$ group is disordered over two orientations. The occupancy factor of the major component of the disorder refines to 0.742(15). CCDC 1430366 contains the supplementary crystallographic data for **6b**.

[Cu(4c)CO] (6c). The structure is ordered. The structure was pseudo-merohedrally twinned. The twin relationship is defined by (101/0-10/00-1), which corresponds to a twofold axis along \mathbf{a}^* . The BASF scale factor refines to 0.3341(9). CCDC 1430367 contains the supplementary crystallographic data for 6c

[Cu(4d)CO] (6d). The structure is ordered. The Cu complex is found at sites of threefold axial symmetry, and only one third of the complex is crystallographically independent. The

absolute configuration was established by anomalous-dispersion effects in diffraction measurements on the crystal. The Flack and Hooft parameters refine to -0.009(6) and -0.010(6),

respectively. CCDC 1430368 contains the supplementary crystallographic data for 6d.

Dalton Transactions

[Cu(4f)CO] (6f). The structure is mostly ordered. One -CF₃ group is disordered over two orientations. The occupancy factor of the major component of the disorder refines to 0.879(14). The crystal that was mounted on the diffractometer was non-merohedrally twinned. The twin relationship corresponds to a twofold axis around 0.9995a* + 0.0115b* + 0.0288c*. The BASF scale factor refines to 0.5073(14). CCDC 1430369 contains the supplementary crystallographic data for 6f.

Ligand and complex synthesis

5-(4-Nitrophenyl)-3-(trifluoridomethyl)-1H-pyrazole (3a). 2a (19.6 g, 75 mmol) was suspended in 250 mL EtOH and the suspension was cooled to 0 °C using an ice bath. Hydrazine hydrate (3.9 mL, 80 mmol) was added dropwise with vigorous stirring. After stirring at 0 °C for 10 minutes the ice bath was removed and the reaction was stirred at room temperature for approx. 30 minutes, the reaction was then heated to reflux for approx. 17 hours. The EtOH was then evaporated in vacuo to a volume of approx. 100 mL. The solution was cooled in an ice bath to 0 °C and 20 mL 37% HCl was added dropwise with vigorous stirring. The solution was left to stir for 1 hour and then poured into 600 mL cold water, the resulting suspension was filtered and the residue was washed on the filter with 1 L water. The solids were dried in vacuo and then purified by vacuum sublimation (215 °C, 10⁻⁴ atm) to yield the product as yellow needles. Yield 14.0 g (73%). M.p. darkened around 150 °C, melted 169–171 °C. 1 H NMR (400 MHz, Acetone- d_{6}) δ 13.53 (s, 1H), 8.35 (d, J = 8.6 Hz, 2H), 8.12 (d, J = 8.6 Hz, 2H), 7.31 (s, 1H). ¹³C NMR (75 MHz, Acetone- d_6) δ 148.71, 144.53 (q, J = 37.6 Hz), 143.30, 135.14, 127.47, 125.27, 122.56 (q, J = 37.6 Hz)267.7 Hz), 103.70.

3-(Trifluoridomethyl)-5-[4-(trifluoridomethyl)phenyl]-1H-pyrazole (3b). 2b (13.3 g, 56 mmol) was dissolved in 26 mL EtOH and 2.2 mL 37% HCl and the solution was cooled to 0 °C with an ice bath. Hydrazine hydrate (1.35 mL, 27.9 mmol) was then slowly added. When the addition was complete the ice bath was removed and the reaction was allowed to stir at room temperature for 20 minutes, it was then heated to reflux for approximately 20 hours. The solvent was removed in vacuo and the resulting solids were purified by vacuum sublimation (140 °C, 10⁻⁴ atm) to yield the product as a white solid. Yield 5.73 g (77%). M.p. 143–145 °C. 1 H NMR (300 MHz, DMSO- d_{6}) δ 13.58 (s, 1H), 7.82–7.55 (m, 4H), 6.74 (s, 1H). ¹³C NMR (100 MHz, Acetone- d_6) δ 149.24, 143.44 (q, J = 38.1 Hz), 134.36, 131.37 (q, J = 34.6), 130.48, 125.12, 124.07 (q, J = 272.5 Hz), 121.36 (q, *J* = 269.3 Hz), 106.38 (q, *J* = 2.3 Hz), 86.82.

5-(4-Chloridophenyl)-3-(trifluoridomethyl)-1*H*-pyrazole (3c). In a flame-dried 500 mL round bottom flask (kept under argon) potassium tert-butoxide (13.5 g, 120 mmol) was suspended in 125 mL dry Et₂O under a dry atmosphere. The sus-

pension was cooled to 0 °C on an ice bath and ethyl trifluoridoacetate (14.2 mL, 119 mmol) was then added dropwise. 4'-Chloridoacetophenone (13 mL, 100 mmol) in 125 mL dry Et₂O was then slowly dropped into the first suspension with vigorous stirring. The ice bath was removed and the reaction was stirred at room temperature for 30 minutes, the reaction was then warmed to 50 °C and stirred overnight. The mixture was added to 250 mL 0.5 M HCl and separated. The aqueous fraction was extracted twice with Et_2O (2 × 125 mL). The combined organic fraction was then washed with water (1 × 200 mL) and brine (1 × 200 mL) and dried over Na₂SO₄. The solvent was removed in vacuo to yield 2c as a yellow solid. Yield 23.4 g (93%). H NMR (400 MHz, CDCl₃) δ 14.57 (s, 1H, enol-OH), 7.87 (d, J = 8.8 Hz, 2H), 7.47 (d, J = 8.8 Hz, 2H), 6.53 (s, 1H). ¹³C NMR (100 MHz, CDCl₃) δ 185.00, 177.42 (q, J = 36.6 Hz), 140.75, 131.39, 129.50, 129.02, 117.22 (q, J = 283.5 Hz), 92.39 (q, J = 2.1 Hz).

2c (23.0 g, 93.4 mmol) was dissolved in 100 mL n-PrOH and hydrazine hydrate (5.0 mL, 103 mmol) was added dropwise. The reaction was heated to reflux for 2 hours. The reaction was then cooled to 0 °C in an ice bath. 10.5 mL 37% HCl was added after which the ice bath was removed and the reaction was heated to 100 °C for 30 minutes. The reaction was cooled down to room temperature and the mixture was diluted with 600 mL cold water. The product was collected by filtration and washed with water (approx. 1 L). The product was dried in vacuo and purified by vacuum sublimation (160 °C, 10^{-4} atm) to yield the product as a white solid. Yield 20.4 g (88%). M.p. 151–153 °C. ¹H NMR (300 MHz, CDCl₃) δ 13.09 (s, 1H), 7.46 (d, J = 8.6 Hz, 2H), 7.38 (d, J = 8.5 Hz, 2H), 6.64 (s, 1H). ¹³C NMR (75 MHz, CDCl₃) δ 144.55, 143.45 (q, J = 37.2 Hz), 135.62, 129.59, 126.87, 126.26, 120.97 (q, J = 268.9 Hz), 101.23 (q, J = 1.6 Hz).

5-(4-Fluoridophenyl)-3-(trifluoridomethyl)-1*H*-pyrazole (3d). 2d (13.25g, 56.6 mmol) was dissolved in 100 mL EtOH and cooled in an ice bath to 0 °C. Hydrazine hydrate (3.25 mL, 67 mmol) was added dropwise. When the addition was complete the ice bath was removed and the reaction was stirred at room temperature for 1 hour and then heated to reflux overnight. The solvent was removed in vacuo to approx. 25 mL. The solution was cooled to 0 °C in an ice bath and slowly 20 mL 37% HCl was added. The ice bath was removed and the reaction was heated to reflux for 1 hour after which the reaction mixture was poured into 150 mL cold water. The product was filtered off, dried in vacuo and purified by vacuum sublimation (100 °C, 10^{-4} atm) to yield the product as an off-white solid. Yield 10.95 g (85%). M.p. 115-118 °C. ¹H NMR (300 MHz, CDCl₃) δ 11.32 (s, 1H), 7.53 (dd, J = 8.8, 5.1 Hz, 2H), 7.13 (t, J = 8.6 Hz, 2H), 6.67 (s, 1H). 13 C NMR (100 MHz, aceton- d_6) δ 163.45 (d, J = 250.1 Hz), 144.64, 143.53 (q, J = 38.6 Hz), 127.65 (d, J = 8.4 Hz), 124.18, 121.05 (q, J = 268.7 Hz), 116.51(d, J = 22.1 Hz), 101.01 (q, J = 1.8 Hz).

5-(4-Methoxyphenyl)-3-(trifluoridomethyl)-1*H*-pyrazole (3f). 2f (22.0 g, 89.3 mmol) was dissolved in 250 mL EtOH and cooled to 0 °C in an ice bath. Hydrazine hydrate (5.0 mL, 103 mmol) was added dropwise with vigorous stirring. The

100.36 (q, J = 2.0 Hz), 55.50.

reaction was stirred at 0 °C for 30 minutes and then heated to reflux overnight. The EtOH was removed *in vacuo* to a volume of approx. 100 mL and the solution was cooled to 0 °C in an ice bath. 10 mL 37% HCl was slowly added and the reaction was heated to reflux for 1 hour after which the mixture was poured into 500 mL cold water. The product was collected by filtration and was recrystallized from EtOH/water at -20 °C to yield transparent needles. Yield 19.66 g (91%). M.p. 134–136 °C. ¹H NMR (400 MHz, CDCl₃) δ 11.55 (s, 1H), 7.49 (d, J = 8.7 Hz, 2H), 6.95 (d, J = 8.7 Hz, 2H), 6.63 (s, 1H), 3.85 (s, 3H). 13 C NMR (100 MHz, CDCl₃) δ 160.50, 145.04, 143.62 (q, J = 38.4 Hz), 127.20, 121.36 (q, J = 268.9 Hz), 120.83, 114.71,

N,N-Dimethyl-4-[3-(trifluoridomethyl)-1H-pyrazol-5-yl]aniline (3g). In a flame-dried 250 mL round bottom flask (kept under argon) potassium tert-butoxide (8.5 g, 75.8 mmol) was suspended in 70 mL dry Et₂O. The suspension was cooled to 0 °C on an ice bath and ethyl trifluoridoacetate (9.0 mL, 75.6 mmol) was slowly added. 4-Acetyl-N,N-dimethylaniline (8.16 g, 50 mmol) was then added in small scoops with vigorous stirring resulting in a clear solution after the last scoop was added. When the addition was complete the reaction was stirred at 0 °C for 45 minutes, the ice bath was then removed and the reaction was allowed to warm to room temperature and stirred until TLC (silica, 5% MeOH in DCM) showed complete consumption of the starting material (approx. 90 minutes). The reaction mixture was then diluted with 30 mL Et₂O and 100 mL 1 M HCl and the layers were separated. The aqueous layer was extracted with Et₂O (1 × 50 mL, 2×25 mL) and the combined organic layers were washed with water $(2 \times 25 \text{ mL})$ and brine $(1 \times 25 \text{ mL})$. The organic fraction was then dried over Na₂SO₄ and evaporated to dryness in vacuo resulting in a red oil that crystallized upon standing to yield 2g as red needles. Yield 12.7 g (98%). ¹H NMR (400 MHz, CDCl₃) δ 15.27 (s, 1H, enol-OH), 7.86 (d, J = 9.1 Hz, 2H), 6.71 (d, J = 9.1Hz, 2H), 6.43 (s, 1H), 3.11 (s, 6H). ¹³C NMR (75 MHz, Acetone d_6) δ 187.41, 174.47 (q, J = 35.1 Hz), 155.7, 131.24, 119.50, 118.84 (q, J = 281.8 Hz), 112.12, 91.15 (q, J = 2.3 Hz), 40.08.

2g (12.7 g, 50 mmol) was dissolved in 125 mL EtOH and cooled to 0 °C in an ice bath. Hydrazine hydrate (2.7 mL, 56 mmol) was added dropwise, when the addition was complete the ice bath was removed and the reaction was stirred at room temperature for 30 minutes before the reaction was heated to reflux for approx. 17 hours. The solvent was evaporated in vacuo and 100 mL 3 M HCl was added. The solution was heated to reflux for 5 minutes, cooled to room temperature and diluted with 500 mL aqueous saturated NaHCO3 solution and 100 mL DCM. The layers were separated and the aqueous fraction was extracted with DCM (2 × 50 mL). The combined organic fractions were washed with water (2 × 100 mL) and brine (1 × 100 mL) and dried over Na₂SO₄. The solvent was removed in vacuo and the product was recrystallized from hot MeOH/water to yield a white solid. Yield (10.2 g, 80%). M.p. 179–181 °C. ¹H NMR (300 MHz, DMSO) δ 12.03 (s, 1H), 7.45 (d, J = 8.9 Hz, 2H), 6.73 (d, J = 8.9 Hz, 2H), 6.62 (s, 1H), 3.00 (s, 1H)6H). ¹H NMR (300 MHz, Acetone- d_6) δ 12.86 (s, 1H), 7.66 (d, J =

9.1 Hz, 2H), 6.85–6.78 (m, 3H), 3.00 (d, J = 1.6 Hz, 6H). ¹³C NMR (75 MHz, CDCl₃) δ 151.07, 145.70, 143.79 (q, J = 35.7 Hz), 126.79, 121.54 (q, J = 268.9 Hz), 115.91, 112.44, 99.50, 40.35.

Sodium hydridobis[3-(trifluoridomethyl)-5-(4-nitrophenyl)pyrazol-1-vl [3-(4-nitrophenyl)-5-(trifluoridomethyl)-pyrazol-1yl]borate (Na4a'). 3a (3.00 g, 11.67 mmol) and NaBH₄ (126 mg, 3.33 mmol) are mixed in 10 mL 4-methylanisole and were placed under argon in a flame-dried Schlenk vessel fitted with a flame dried glass tube (30 cm). The mixture was heated to 120 °C for 2 hours to form the di-substituted borate species, bubbling was observed using an oil bubbler and became sporadic after approx. 90 minutes. The temperature was then raised to 180 °C for three hours. After approx. 1.5 hours bubbling stopped but BH₄ was still observed on ¹H NMR, after 3 hours BH₄ was no longer observed. The solvent was then removed in vacuo to yield the product as a brown oil. The product was purified by extensive trituration with Et2O to yield the product as an off-white solid which was recrystallized from DCM/pentane. Yield 1.11 g (40%). M.p. 225 °C (decomposition). ¹H NMR (500 MHz, CD_2Cl_2) δ 8.19 (d, J = 8.4 Hz, 2H), 8.05 (d, J = 8.3 Hz, 4H), 7.77 (d, J = 8.4 Hz, 2H), 7.32 (d, J =8.3 Hz, 4H), 6.97 (s, 1H), 6.66 (s, 2H), 4.59 (bs, 1H). ¹³C NMR (75 MHz, acetone- d_6) δ 150.17, 148.75, 148.06, 147.82, 143.21 (q, J = 36.8 Hz), 140.64, 139.37, 138.63 (q, J = 38.1 Hz), 130.98,127.09, 124.57, 123.50, 123.15 (q, J = 267.6 Hz), 121.73 (q, J = 267.6 Hz) 269.0 Hz), 106.79 (q, J = 3.0 Hz), 105.73 (q, J = 1.8 Hz). HRMS (ESI neg.) m/z calcd For [M⁻] (= $C_{30}H_{16}BF_9N_9O_6^-$) 780.11674 found 780.11778.

hydrotris[3-(trifluoridomethyl)-5-(4-{trifluorido-**Sodium** methyl}phenyl)pyrazol-1-yl]borate (Na4b). 3b (7.75)27.7 mmol) and NaBH₄ (0.202 g, 5.35 mmol) were mixed and placed under argon in a flame-dried Schlenk vessel fitted with a flame-dried condenser (not cooled with water). The mixture was heated 200 °C for 4 hours, 3b subliming in the glassware was occasionally molten using a heat gun to return it to the reaction mixture. The remaining pyrazole was removed from the product by extensive vacuum sublimation at 160 °C. The product was dissolved in DCM and filtered over celite to remove insoluble byproducts. The solvent was removed in vacuo to yield the product as a white powder. Yield 3.59 g (77%). M.p. 212–214 °C. ¹H NMR (300 MHz, acetone- d_6) δ 7.37 (d, J = 8.4 Hz, 6H), 7.23 (d, J = 8.4 Hz, 6H), 6.74 (s, 3H), 4.47(bs, 1H). ¹³C NMR (75 MHz, acetone- d_6) δ 150.38, 143.75 (q, J =36.7 Hz), 136.43, 131.05, 125.36 (m), 122.97 (q, J = 267.7 Hz), 125.25 (q, J = 271.8 Hz), 105.34 (q, J = 1.9 Hz). HRMS (ESI neg.) m/z calcd For [M⁻] (= $C_{33}H_{16}BF_{18}N_6^-$) 849.12366 found

Sodium hydrotris[3-(trifluoridomethyl)-5-(4-chloridophenyl)-pyrazol-1-yl]borate (Na4c). 3c (5.00 g, 20.3 mmol) and NaBH₄ (0.247 g, 6.53 mmol) were placed in a flame-dried Schlenk vessel fitted with a flame-dried glass tube (30 cm) and placed under argon. The mixture was heated at once to 180 °C and held at this temperature for 2.5 hours. The condenser was then replaced with a cold finger and vacuum was applied (10^{-4} atm). The pyrazole was left to sublime out of the product over-

night. When no more of the pyrazole deposited on the cold finger the cold finger was removed and the product was dissolved in THF (approx. 50 mL) and filtered over celite to remove insoluble byproducts. The THF was evaporated in vacuo and the resulting solids were washed with boiling heptane (4 × 20 mL) and Et₂O (1 × 20 mL) on a glass frit leaving the pure product as a 1:1 mixture of the Et₂O and THF adducts. Yield 3.2 g (62%). M.p. 192 °C (decomposition). ¹H NMR (400 MHz, CDCl₃) δ 7.00 (d, J = 8.4 Hz, 6H), 6.77 (d, J =8.4 Hz, 6H), 6.44 (s, 3H), 4.57 (bs, 1H), 3.92 (ddd, J = 6.5, 4.2, 2.7 Hz, 2H, coord. THF), 3.55 (q, J = 7.0 Hz, 2H, coord. Et₂O), 2.02-1.96 (m, 2H, coord. THF), 1.24 (t, J = 7.0 Hz, 3H, coord. Et₂O). ¹³C NMR (100 MHz, Acetone-d₆) δ 150.38, 143.25, 134.56, 131.69, 131.07, 128.52, 121.44, 104.67. HRMS (ESI neg.) m/z calcd For [M⁻] (= $C_{30}H_{16}BCl_3F_9N_6^-$) 747.04459 found 747.04770.

Dalton Transactions

Sodium hydrotris[3-(trifluoridomethyl)-5-(4-fluoridophenyl)pyrazol-1-yl]borate (Na4d). 3d (5.00 g, 21.7 mmol) and NaBH₄ (0.267 g, 7.06 mmol) were placed in a flame-dried Schlenk vessel fitted with a flame dried glass tube (30 cm) and placed under argon. The mixture was heated to 180 °C for 3 hours and 20 minutes. The temperature was lowered to 140 °C and the condenser was replaced with a cold finger, leftover pyrazole was removed by vacuum sublimation. When no more pyrazole deposited on the cold finger the residue was dissolved in toluene (50 mL) and filtered over celite to remove insoluble byproducts. The toluene was evaporated in vacuo and the remaining solids were dissolved in acetone and evaporated to dryness. Yield 1.72 g (53%). M.p. 190 °C (decomposition). ¹H NMR (400 MHz, CDCl₃) δ 6.88 (dd, J = 8.6, 5.4 Hz, 6H), 6.72 (t, J = 8.6 Hz, 6H, 6.44 (s, 3H), 4.61 (bs, 1H), 2.34 (s, 6H, coord.)acetone). 13 C NMR (100 MHz, CDCl₃) δ 220.47 (coord. acetone), 162.75 (d, J = 248.1 Hz), 150.18, 142.70 (q, J =36.6 Hz), 131.60 (d, J = 8.3 Hz), 127.79 (d, J = 3.3 Hz), 122.20 (d, J = 267.8 Hz), 114.74 (d, J = 21.7 Hz), 103.84 (q, J = 1.5 Hz),65.98 (coord. THF), 31.31 (coord. acetone), 23.06 (coord. THF). HRMS (ESI neg.) m/z calcd for [M⁻] (= $C_{30}H_{16}BF_{12}N_6^-$) 699.13324 found 699.13033.

Sodium hydrotris[3-(trifluoridomethyl)-5-(4-methoxyphenyl)pyrazol-1-yl]borate (Na4f). 3f (6.867 g, 28.35 mmol) and NaBH₄ (0.346 g, 9.15 mmol) were placed in a flame-dried Schlenk vessel fitted with a flame-dried glass tube (30 cm) and placed under argon. The mixture was heated to 180 °C for 3 hours. The product was dissolved in boiling toluene (50 mL) and filtered, the filtrate was diluted with 200 mL heptane and left to stand while the product crystallized. Filtration yielded a white powder. Recrystallization from acetone yielded the product as its acetone adduct. Yield 3.75 g (53%). M.p. 206 °C (decomposition). ¹H NMR (300 MHz, CDCl₃) δ 6.85 (d, J = 8.6 Hz, 6H), 6.52 (d, J = 8.6 Hz, 6H), 6.42 (s, 3H), 4.69 (bs, 1H), 3.79 (s, 9H), 2.33 (s, coord. acetone). ¹³C NMR (75 MHz, CDCl₃) δ 212.24 (coord. Acetone), 159.40, 151.06, 142.34 (q, J = 36.2 Hz), 131.26, 122.37 (q, J = 268.0 Hz), 113.08, 103.10 (q, J = 268.0 Hz) 1.6 Hz), 55.14, 31.27 (coord. acetone). HRMS (ESI neg.) m/z calcd for [M⁻] (= $C_{33}H_{25}BF_9N_6O_3^-$) 735.19320 found 735.19424.

Sodium hydrotris[3-(trifluoridomethyl)-5-(4-{N,N-dimethylamino}phenyl)pyrazol-1-yl]borate (Na4g). 3g 23.5 mmol) and NaBH₄ (0.286 g, 7.56 mmol) were suspended in 20 mL 4-methylanisole in a flame dried Schlenk flask fitted with a flame-dried glass tube (30 cm) and placed under argon. The mixture was heated to reflux for 4 hours. The mixture was allowed to cool to room temperature and 200 mL petroleum ether was added. The diluted mixture was stirred in an ice bath for approx. 30 minutes and then filtered. The filtrate was washed with MeCN (6 × 25 mL) and then dissolved in acetone (50 mL). The acetone was removed in vacuo to yield the product as a white powder. The product formed was the acetone adduct. Yield 1.80 g (28%). Decomposed around 230 °C. ¹H NMR (300 MHz, Acetone- d_6) δ 6.82 (d, I = 8.9 Hz, 6H), 6.46 (s, 3H), 6.33 (d, J = 8.9 Hz, 6H), 4.93 (bs, 1H), 2.93 (s, 18H). ¹³C NMR (75 MHz, CDCl₃) δ 152.86, 150.81, 142.83 (q, J = 36.1 Hz), 131.28, 123.37 (q, J = 267.4 Hz), 120.35, 112.07, 103.18 (q, J = 1.8 Hz), 40.22. HRMS (ESI neg.) m/z calcd for $[M^{-}]$ (= $C_{36}H_{34}BF_{9}N_{9}^{-}$) 774.28810 found 774.28907.

General method for synthesis of the copper(i) ethene complexes (5a', 5b-g)

Na4a' or Na4b–g (50 mg) was dissolved in 5 mL dry, degassed DCM. The solution was bubbled with ethene for 2 minutes. CuI (1.05 eq.) was then added and the solution was saturated/bubbled with ethene for another 2 minutes. The flask was then stoppered and left to stir at medium speed overnight to form a white suspension. The suspension was filtered using a syringe filter (0.45 μ m PTFE) and the solvent was removed *in vacuo* to yield the products as white powders. The complexes could be further purified by recrystallization from DCM/pentane at -20 °C under an ethene atmosphere to yield colorless blocks except for 5a' which was brown.

[Cu(4a')(C₂H₄)] (5a'). Yield 42 mg (83%), yellow solid. 1 H NMR (300 MHz, CD₂Cl₂) δ 8.37 (d, J = 8.9 Hz, 2H), 8.07 (d, J = 8.9 Hz, 4H), 7.76 (d, J = 8.9 Hz, 2H), 7.36 (d, J = 8.9 Hz, 4H), 6.87 (s, 1H), 6.72 (s, 2H), 4.54 (bs, 1H), 4.44 (s, 4H). 13 C NMR (126 MHz, CD₂Cl₂) δ 152.46, 148.84, 148.67, 148.42, 143.52 (q, J = 38.4 Hz), 139.00 (q, J = 39.1 Hz), 138.60, 136.99, 131.11, 129.57, 124.32, 123.36, 121.23 (q, J = 269.3 Hz), 120.05 (q, J = 269.7 Hz), 106.76 (q, J = 2.5 Hz), 86.37. Elemental analysis calc. (%) for C_{32} H₂₀BCuF₉N₉O₆·1.5H₂O·1.0DCM (found): C 40.29 (41.20), H 2.56 (2.8), N 12.81 (12.32).

[Cu(4b)(C₂H₄)] (5b). Yield 49 mg (91%). ¹H NMR (400 MHz, CD₂Cl₂) δ 7.22 (d, J = 8.4 Hz, 6H), 7.00 (d, J = 8.3 Hz, 6H), 6.69 (s, 3H), 4.96 (s, 4H), 4.43 (bs, 1H). ¹³C NMR (100 MHz, CD₂Cl₂) δ 149.24, 143.44 (q, J = 38.2 Hz), 134.36, 131.37 (q, J = 33.8 Hz), 130.48, 125.12, 124.07 (q, J = 272.4 Hz), 121.36 (q, J = 269.3 Hz), 106.38 (q, J = 2.4 Hz), 86.82. Elemental analysis calc. (%) for C₃₅H₂₀BCuF₁₈N₆ (found): C 44.68 (44.63), H 2.14 (2.01), N 8.93 (8.91).

[Cu(4c)(C₂H₄)] (5c). Yield 47 mg (94%). ¹H NMR (600 MHz, CD₂Cl₂) δ 7.02 (d, J = 8.5 Hz, 6H), 6.80 (d, J = 8.5 Hz, 6H), 6.61 (s, 3H), 4.92 (s, 4H), 4.47 (bs, 1H). ¹³C NMR (151 MHz, CD₂Cl₂) δ 149.57, 143.14 (q, J = 38.0 Hz), 135.49, 131.41, 129.26, 128.49, 121.45 (q, J = 269.0 Hz), 105.93 (q, J = 2.5 Hz), 86.35. Elemental

analysis calc. (%) for $C_{32}H_{20}BCl_3CuF_9N_6$ (found): C 45.74 (46.37), H 2.40 (2.77), N 10.00 (9.87).

[Cu(4d)(C₂H₄)] (5d). Yield 36.6 mg (73%). ¹H NMR (300 MHz, CD₂Cl₂) δ 6.95–6.83 (m, 6H), 6.74 (t, J = 8.5 Hz, 6H), 6.60 (s, 3H), 4.91 (s, 4H), 4.54 (bs, 1H). ¹³C NMR (126 MHz, CD₂Cl₂) δ 163.24 (d, J = 249.8 Hz), 149.65, 142.95 (q, J = 37.9 Hz), 131.86 (d, J = 8.3 Hz), 126.88 (d, J = 3.4 Hz), 121.41 (q, J = 268.7 Hz), 115.13 (d, J = 21.6 Hz), 105.92 (q, J = 2.4 Hz), 86.07. Elemental analysis calc. (%) for C₃₂H₂₀BCuF₁₂N₆·H₂O (found): C 47.52 (47.48), H 2.74 (2.57), N 10.39 (10.23).

[Cu(4f)(C₂H₄)] (5f). Yield 43.5 mg (86%). ¹H NMR (400 MHz, CD₂Cl₂) δ 6.81 (d, J = 8.7 Hz, 6H), 6.56 (s, 3H), 6.51 (d, J = 8.7 Hz, 6H), 4.88 (s, 4H), 4.62 (bs, 1H), 3.78 (s, 9H). ¹³C NMR (100 MHz, CD₂Cl₂) δ 160.29, 150.69, 142.51 (q, J = 37.6 Hz), 131.47, 123.22, 121.67 (q, J = 268.8 Hz), 113.55, 105.25 (q, J = 2.5 Hz), 85.57, 55.47. Elemental analysis calc. (%) for C₃₅H₂₉BCuF₉N₆O₃ (found): C 51.01 (50.83), H 3.47 (3.53), N 10.12 (10.16).

[Cu(4g)(C₂H₄)] (5g). Yield 40 mg (79%). ¹H NMR (500 MHz, CD₂Cl₂) δ 6.75 (d, J = 8.7 Hz, 6H), 6.51 (s, 3H), 6.26 (d, J = 8.7 Hz, 6H), 4.84 (s, 4H), 4.77 (bs,1H), 2.92 (s, 18H). ¹³C NMR (126 MHz, CD₂Cl₂) δ 151.56, 150.56, 142.41 (q, J = 37.5 Hz), 130.98, 121.82 (q, J = 268.6 Hz), 118.42, 111.46, 104.57 (q, J = 2.6 Hz), 84.94, 40.12. Elemental analysis calc. (%) for C₃₈H₃₈BCuF₉N₉·0.2C₅H₁₂ (found): C 53.20 (53.40), H 4.62 (4.61), N 14.32 (14.07).

General method for the synthesis of the copper(ı)-CO complexes (6a', 6b-g)

Na4a' or Na4b–g (50 mg) was dissolved in dry, degassed DCM. The solution was bubbled with argon for 2 minutes and placed in a glass-lined autoclave (volume 12 mL). CuI (1.05 eq.) was added and the autoclave was closed and purged with dry nitrogen gas. The autoclave was then pressurized with carbon monoxide to at least 5 atm and left to stir at room temperature for 20 hours. The autoclave was then bubbled with dry nitrogen gas to remove unreacted carbon monoxide. The resulting white suspension was filtered using a syringe filter (0.45 μ m, PTFE) and the solvent was removed *in vacuo* to leave behind the product as a white powder except in the case of 6a' which was brown

[Cu(4a')(CO)] (6a'). Yield 36 mg (56%). ¹H NMR (300 MHz, CD₂Cl₂) δ 8.40 (d, J = 8.5 Hz, 2H), 8.09 (d, J = 8.5 Hz, 4H), 7.91 (d, J = 8.4 Hz, 2H), 7.35 (d, J = 8.4 Hz, 4H), 6.91 (s, 1H), 6.72 (s, 2H), 4.40 (bs, 1H). ¹³C NMR (100 MHz, CD₂Cl₂) δ 151.85, 149.09, 148.89, 148.66, 143.50 (q, J = 38.1 Hz), 139.41 (q, J = 39.5 Hz), 138.09, 136.57, 131.11, 129.05, 124.53, 123.49, 121.12 (q, J = 269.2 Hz), 119.97 (q, J = 269.5 Hz), 107.27, 106.33. IR (cm⁻¹): 2611 (w, BH stretching), 2105 (s, CO stretching). Elemental analysis calc. (%) for C₃₁H₁₆BCuF₉N₉O₇ (found): C 42.71 (42.88), H 1.85 (1.97), N 14.46 (14.34).

[Cu(4b)(CO)] (6b). Yield 36 mg (86%). ¹H NMR (300 MHz, CD₂Cl₂) δ 7.25 (d, J = 8.4 Hz, 6H), 6.99 (d, J = 8.4 Hz, 6H), 6.69 (s, 3H), 4.29 (bs, 1H). ¹³C NMR (75 MHz, CD₂Cl₂) δ 149.02, 143.00 (q, J = 37.8 Hz), 133.62, 131.20 (q, J = 33.7 Hz), 130.13, 124.82 (tt, J = 3.9, 1.9 Hz), 123.70 (q, J = 277.1 Hz), 120.87 (q,

J = 269.3), 105.24 (q, J = 1.8 Hz). IR (cm⁻¹): 2620 (w, BH stretching), 2120 (s, CO stretching). Elemental analysis calc. (%) for $C_{34}H_{16}BCuF_{18}N_6O$ (found): C 43.40 (43.20), H 1.71 (1.79), N 8.93 (8.83).

[Cu(4c)(CO)] (6c). Yield 45 mg (90%). 1 H NMR (300 MHz, CD₂Cl₂) δ 7.04 (d, J = 8.3 Hz, 6H), 6.79 (d, J = 8.5 Hz, 6H), 6.61 (s, 3H), 4.33 (bs, 1H). 13 C NMR (75 MHz, CD₂Cl₂) δ 149.71, 143.06 (q, J = 37.8 Hz), 135.66, 131.38, 128.85, 128.54, 121.31 (q, J = 269.2 Hz), 105.17 (q, J = 2.0 Hz). IR (cm $^{-1}$): 2616 (w, BH stretching), 2113 (s, CO stretching). Elemental analysis calc. (%) for C₃₁H₁₆BCl₃CuF₉N₆O (found): C 44.31 (44.43), H 1.92 (1.99), N 10.00 (9.95).

[Cu(4d)(CO)] (6d). Yield 34 mg (72%). ¹H NMR (300 MHz, CD₂Cl₂) δ 6.89 (dd, J = 8.9, 5.3 Hz, 6H), 6.76 (dd, J = 9.0, 8.5 Hz, 6H), 6.59 (s, 3H), 4.45 (bs, 1H). ¹³C NMR (75 MHz, CD₂Cl₂) δ 163.41 (d, J = 247.5 Hz), 149.86, 142.92 (q, J = 37.8 Hz), 131.93 (d, J = 8.5 Hz), 126.54 (d, J = 3.5 Hz), 121.34 (q, J = 268.9 Hz), 115.28 (d, J = 21.8 Hz), 105.25 (q, J = 1.8 Hz). IR (cm⁻¹): 2616 (w, BH stretching), 2103 (s, CO stretching). Elemental analysis calc. (%) for C₃₁H₁₆BCuF₁₂N₆O·0.2C₅H₁₂ (found): C 47.73 (48.03), H 2.30 (2.30), N 10.44 (10.65).

[Cu(4f)(CO)] (6f). Yield 45 mg (89%). 1 H NMR (300 MHz, CD₂Cl₂) δ 6.79 (d, J = 8.6 Hz, 6H), 6.55 (s, 3H), 6.52 (d, J = 8.7 Hz, 6H), 4.50 (bs, 1H), 3.79 (s, 9H). 13 C NMR (75 MHz, CD₂Cl₂) δ 160.07, 150.46, 142.24 (q, J = 37.3 Hz), 131.11, 122.45, 121.18 (q, J = 269.0 Hz), 113.23, 104.12 (q, J = 1.8 Hz), 55.17. IR (cm⁻¹): 2636 (w, BH stretching), 2096 (s, CO stretching). Elemental analysis calc. (%) for $C_{34}H_{25}BCuF_{9}N_{6}O_{4}$ (found): C 49.38 (49.11), H 3.05 (3.14), N 10.16 (9.99).

[Cu(4g)(CO)] (6g). Yield 51 mg (86%). ¹H NMR (300 MHz, CD₂Cl₂) δ 6.74 (d, J = 8.8 Hz, 6H), 6.50 (s, 3H), 6.28 (d, J = 8.8 Hz, 6H), 4.66 (bs, 1H), 2.92 (s, 18H). ¹³C NMR (75 MHz, CD₂Cl₂) δ 151.32, 150.34, 142.14, 130.62, 117.65, 111.12, 103.41 (q, J = 1.8 Hz), 40.15. CO and CF₃ could not resolved due to the low solubility of the complex. IR (cm⁻¹): 2647 (w, BH stretching), 2096 (s, CO stretching). Elemental analysis calc. (%) for C₃₇H₃₄BCuF₉N₉O·H₂O (found): C 50.27 (50.63), H 4.10 (4.24), N 14.26 (13.90).

Acknowledgements

This work is supported by NanoNextNL, a micro and nanotechnology consortium of the Government of the Netherlands and 130 partners. We thank Jos van Brussel for CHN analysis; Gerwin Spijksma for HRMS and Fons Lefeber and Karthick Sai Sankar Gupta are acknowledged for assistance with the NMR experiments.

References

- 1 For an explanation of the nomenclature of poly(pyrazolyl)-borates see p. 5 of ref. 4.
- 2 S. Trofimenko, J. Am. Chem. Soc., 1966, 88, 1842–1844.
- 3 S. Trofimenko, J. Am. Chem. Soc., 1967, 89, 3170-3177.

4 S. Trofimenko, Scorpionates: The Coordination Chemistry of

- Poly(pyrazolyl)borate Ligands, Imperial College Press, London, 1999.
- 5 C. Pettinari, Scorpionates II: Chelating Borate Ligands, Imperial College Press, London, 2008.
- 6 S. Trofimenko, Chem. Rev., 1993, 93, 943-980.

Dalton Transactions

- 7 H. V. R. Dias and C. J. Lovely, Chem. Rev., 2008, 108, 3223-3238.
- 8 N. Kitajima, K. Fujisawa, C. Fujimoto, Y. Morooka, S. Hashimoto, T. Kitagawa, K. Toriumi, K. Tatsumi and A. Nakamura, J. Am. Chem. Soc., 1992, 114, 1277-1291.
- 9 M. A. Casado, V. Hack, J. A. Camerano, M. A. Ciriano, C. Tejel and L. A. Oro, Inorg. Chem., 2005, 44, 9122-
- 10 B. S. Hammes, M. W. Carrano and C. J. Carrano, J. Chem. Soc., Dalton Trans., 2001, 1448-1451.
- 11 J. C. Calabrese, P. J. Domaille, S. Trofimenko and G. J. Long, Inorg. Chem., 1991, 30, 2795-2801.
- 12 C. Pérez Olmo, K. Böhmerle, G. Steinfeld and H. Vahrenkamp, Eur. J. Inorg. Chem., 2006, 2006, 3869-3877.
- 13 S. Kealey, N. J. Long, P. W. Miller, A. J. P. White and A. D. Gee, Dalton Trans., 2008, 2677-2679.
- 14 E. I. Solomon, D. E. Heppner, E. M. Johnston, J. W. Ginsbach, J. Cirera, M. Qayyum, M. T. Kieber-Emmons, C. H. Kjaergaard, R. G. Hadt and L. Tian, Chem. Rev., 2014, 114, 3659-3853.
- 15 X. Kou, J. Wu, T. R. Cundari and H. V. R. Dias, Dalton Trans., 2009, 915-917.
- 16 H. V. R. Dias and T. Goh, Polyhedron, 2004, 23, 273-
- 17 N. B. Javaratna, I. I. Gerus, R. V. Mironets, P. K. Mykhailiuk, M. Yousufuddin and H. V. R. Dias, Inorg. Chem., 2013, 52, 1691-1693.
- 18 H. V. R. Dias, H.-J. Kim, H.-L. Lu, K. Rajeshwar, N. R. de Tacconi, A. Derecskei-Kovacs and D. S. Marynick, Organometallics, 1996, 15, 2994-3003.
- 19 C. Hansch, A. Leo and R. W. Taft, Chem. Rev., 1991, 91, 165-195.
- 20 H. V. R. Dias, H. L. Lu, H. J. Kim, S. A. Polach, T. Goh, R. G. Browning and C. J. Lovely, Organometallics, 2002, 21, 1466-1473.

- 21 W. A. King, G. P. A. Yap, C. D. Incarvito, A. L. Rheingold and K. H. Theopold, Inorg. Chim. Acta, 2009, 362, 4493-
- 22 R. Shannon, Acta Crystallogr., Sect. A: Cryst. Phys., Diffr., Theor. Gen. Cryst., 1976, 32, 751-767.
- 23 H. Plenio, Chem. Rev., 1997, 97, 3363-3384.
- 24 C. Martín, J. M. a. Muñoz-Molina, A. Locati, E. Alvarez, F. Maseras, T. s. R. Belderrain and P. J. Pérez, Organometallics, 2010, 29, 3481-3489.
- 25 H. V. R. Dias, X. Y. Wang and H. V. K. Diyabalanage, Inorg. Chem., 2005, 44, 7322-7324.
- 26 J. S. Thompson, R. L. Harlow and J. F. Whitney, J. Am. Chem. Soc., 1983, 105, 3522-3527.
- 27 T. J. Marks and J. R. Kolb, Chem. Rev., 1977, 77, 263-293.
- 28 K. Fujisawa, T. Ono, Y. Ishikawa, N. Amir, Y. Miyashita, K.-i. Okamoto and N. Lehnert, Inorg. Chem., 2006, 45, 1698-1713.
- 29 M. Kujime, T. Kurahashi, M. Tomura and H. Fujii, Inorg. Chem., 2007, 46, 541-551.
- 30 J. L. Duncan, Mol. Phys., 1974, 28, 1177-1191.
- 31 W. Gordy, Microwave Spectroscopy, Wiley, New York, 1953.
- 32 H. V. R. Dias and H.-L. Lu, Inorg. Chem., 1995, 34, 5380-5382.
- 33 K. Fujisawa, M. Yoshida, Y. Miyashita and K.-i. Okamoto, Polyhedron, 2009, 28, 1447-1454.
- 34 M. I. Bruce and A. P. P. Ostazewski, J. Chem. Soc., Dalton Trans., 1973, 2433-2436.
- 35 Unpublished results.
- 36 M. Pellei, G. Papini, G. G. Lobbia, S. Ricci, M. Yousufuddin, H. V. Rasika Dias and C. Santini, Dalton Trans., 2010, 39, 8937-8944.
- 37 M. Cano, J. V. Heras, S. Trofimenko, A. Monge, E. Gutierrez, C. J. Jones and J. A. McCleverty, J. Chem. Soc., Dalton Trans., 1990, 3577-3582.
- 38 G. R. Fulmer, A. J. M. Miller, N. H. Sherden, H. E. Gottlieb, A. Nudelman, B. M. Stoltz, J. E. Bercaw and K. I. Goldberg, Organometallics, 2010, 29, 2176-2179.
- 39 S. Büttner, A. Riahi, I. Hussain, M. A. Yawer, M. Lubbe, A. Villinger, H. Reinke, C. Fischer and P. Langer, Tetrahedron, 2009, 65, 2124-2135.
- 40 G. Sheldrick, Acta Crystallogr., Sect. A: Fundam. Crystallogr., 2008, 64, 112-122.